

# TIM-1 and TIM-4 Glycoproteins Bind Phosphatidylserine and Mediate Uptake of Apoptotic Cells

Norimoto Kobayashi,<sup>1</sup> Piia Karisola,<sup>2</sup> Victor Peña-Cruz,<sup>1</sup> David M. Dorfman,<sup>3</sup> Masahisa Jinushi,<sup>1</sup> Sarah E. Umetsu,<sup>4</sup> Manish J. Butte,<sup>5</sup> Haruo Nagumo,<sup>1</sup> Irene Chernova,<sup>1</sup> Baogong Zhu,<sup>1</sup> Arlene H. Sharpe,<sup>5</sup> Susumu Ito,<sup>6</sup> Glenn Dranoff,<sup>1</sup> Gerardo G. Kaplan,<sup>7</sup> Jose M. Casasnovas,<sup>8</sup> Dale T. Umetsu,<sup>2</sup> Rosemarie H. DeKruyff,<sup>2</sup> and Gordon J. Freeman<sup>1,\*</sup>

<sup>1</sup>Department of Medical Oncology, Dana-Farber Cancer Institute, 44 Binney Street, and Department of Medicine, Harvard Medical School, Boston, MA 02115, USA

<sup>2</sup>Division of Immunology, Children's Hospital Boston, Harvard Medical School, Boston, MA 02115, USA

<sup>3</sup>Department of Pathology, Brigham and Women's Hospital and Harvard Medical School, Boston, MA 02115, USA

<sup>4</sup>Department of Microbiology-Immunology, Northwestern University, Feinberg School of Medicine, Chicago, Illinois 60611

<sup>5</sup>Department of Pathology

<sup>6</sup>Department of Neurobiology

Harvard Medical School, Boston, MA 02115, USA

<sup>7</sup>Center for Biologics Evaluation and Research, Food and Drug Administration, Bethesda, MD 20892, USA

<sup>8</sup>Centro Nacional de Biotecnología, CSIC, Campus Universidad Autónoma, 28049 Madrid, Spain

\*Correspondence: [gordon\\_freeman@dfci.harvard.edu](mailto:gordon_freeman@dfci.harvard.edu)

DOI 10.1016/j.immuni.2007.11.011

## SUMMARY

The T cell immunoglobulin mucin (TIM) proteins regulate T cell activation and tolerance. Here we showed that TIM-4 is expressed on human and mouse macrophages and dendritic cells, and both TIM-4 and TIM-1 specifically bound phosphatidylserine (PS) on the surface of apoptotic cells but not any other phospholipid tested. TIM-4<sup>+</sup> peritoneal macrophages, TIM-1<sup>+</sup> kidney cells, and TIM-4- or TIM-1-transfected cells efficiently phagocytosed apoptotic cells, and phagocytosis could be blocked by TIM-4 or TIM-1 monoclonal antibodies. Mutations in the unique cavity of TIM-4 eliminated PS binding and phagocytosis. TIM-4 mAbs that blocked PS binding and phagocytosis mapped to epitopes in this binding cavity. These results show that TIM-4 and TIM-1 are immunologically restricted members of the group of receptors whose recognition of PS is critical for the efficient clearance of apoptotic cells and prevention of autoimmunity.

## INTRODUCTION

The T cell immunoglobulin mucin (TIM) gene family was identified as molecules related to higher risk of development of asthma and allergic disease in mice (McIntire et al., 2001). Multiple studies have now confirmed the association of the TIM gene family with development of autoimmunity and allergic diseases (reviewed in Kuchroo

et al., [2006]). TIM-1 and TIM-3 are preferentially expressed on distinct mouse T cell subsets, with TIM-1 being on T helper 2 cells (Th2) (Umetsu et al., 2005) and TIM-3 on Th1 cells (Monney et al., 2002). The TIM gene family includes three members in human and eight in mouse. Human TIM-1, TIM-3, and TIM-4 appear to be the functional orthologs to mouse TIM-1, TIM-3, and TIM-4 (Kuchroo et al., 2003). Mouse TIM-5 and TIM-8 are inferred from genomic sequences and have not yet been characterized. All TIM family proteins are type I cell-surface glycoproteins and share common structural motifs including an immunoglobulin variable (IgV) domain with six cysteines, a mucin-like domain, a transmembrane domain, and a cytoplasmic domain. All TIMs except for TIM-4 contain a tyrosine-kinase phosphorylation motif in the cytoplasmic domain. The TIMs differ in the length of the mucin domain and the number of O-linked glycosylation sites (Kuchroo et al., 2003).

The crystal structures of murine TIM-1, TIM-2, and TIM-3 IgV domains have been described (Cao et al., 2007; Santiago et al., 2007b). TIM-1 and TIM-3 IgV domains display a distinctive cleft formed by the CC' and FG loops of the GFC  $\beta$  sheet. This is the face commonly used by Ig superfamily receptors for ligand binding. This cavity is conserved within the TIM family, except for TIM-2. We have found that in TIM-1 and TIM-4, the narrow cavity built by the CC' and FG loops is a binding site for phosphatidylserine (PS). In the accompanying paper, Santiago et al. (2007a) describe the structure of the co-crystal of PS and mTIM-4.

The redistribution of PS to the outer leaflet of the plasma membrane is a key signal for recognition of apoptotic cells by phagocytes (Fadok et al., 1992; Verhoven et al., 1995). Rapid removal of apoptotic cells by phagocytes is critical

for the maintenance of tolerance and prevents inflammation and autoimmune responses against intracellular antigens released from the dying cells (Savill and Fadok, 2000). Several receptors that participate in the recognition of PS on the surface of apoptotic cells have been identified, and deficiencies of these molecules in mouse models lead to a failure to maintain self-tolerance and development of autoimmunity (Asano et al., 2004; Cohen et al., 2002).

Although several reports of the murine TIM family focused on the interaction between antigen-presenting cells (APCs) and CD4<sup>+</sup> T cells and regulation of Th1 and Th2 balance and tolerance, there are no data on TIM function in phagocytosis or innate immunity. Here we report that TIM-4 is expressed on mature macrophages and dendritic cell (DC) populations in both human and mouse. Our binding assays and the TIM-4 crystal structure (Santiago et al., 2007a) showed binding of PS to TIM-4. TIM-4 mAbs that blocked binding to PS substantially reduced phagocytosis of apoptotic cells by mouse peritoneal macrophages. TIM-4- or TIM-1-transfected 3T3 cells and TIM-1-expressing human kidney epithelial cell lines had increased apoptotic-cell phagocytosis that could be blocked by specific mAbs. These results show that TIM-4 and TIM-1 recognize PS and are important for the efficient clearance of apoptotic cells by antigen presenting cells.

## RESULTS

### TIM-4 and TIM-1 Bind to a Structure Highly Expressed on the Surface of Apoptotic Cells

We prepared Ig fusion proteins with the extracellular domains or the IgV domains of TIM-1, TIM-2, or TIM-4 in order to identify their functional ligands. TIM-4-Ig and TIM-1-Ig bound weakly to all long-term-cultured cell lines tested (data not shown). We noticed that a minor population of each cell line had a much higher intensity of staining with TIM-4-Ig or TIM-1-Ig. On the basis of the side-scatter and forward-scatter gating of the cells, the brightly staining cells appeared to be dead cells (Figure 1A); however, the intensity of staining was much larger than the typical increase in background staining frequently observed on dead cells. We prepared Jurkat cells with a moderate proportion of apoptotic cells by cross-linking CD95 (anti-Fas, IgM), and we stained the Jurkat cells with TIM-4-Ig or TIM-1-Ig as well as annexin V-FITC and propidium iodide to visualize early and late apoptotic cells. TIM-4-Ig bound weakly to live Jurkat cells but strongly to a structure on early and late apoptotic Jurkat cells (Figure 1B).

To further characterize the binding of TIM-1 and TIM-4 to apoptotic cells, we prepared populations with a high proportion of early apoptotic cells. Treatment of Jurkat cells with CD95 mAb, followed by centrifugation on Ficoll to remove late apoptotic cells, gave a population with more than 90% early apoptotic cells as judged by Annexin V-FITC and propidium-iodide staining (Figure 1C). We analyzed the binding of TIM-Ig to these apoptotic cells or to untreated cells. Binding of TIM-Ig was performed in

the absence of annexin-V-FITC and propidium iodide to eliminate any competition or complication by annexin-V binding to PS. Human (h)TIM-4-Ig, hTIM-1-Ig, mouse (m)TIM-4(IgV)-Ig, and mTIM-1(IgV)-Ig bound slightly to live Jurkat cells but strongly to apoptotic Jurkat cells (Figure 1D).

Red blood cells (RBCs) can be induced to undergo an apoptotic-like process, termed eryptosis, by incubation with ionomycin and phorbol ester. Eryptotic RBCs expose PS on the RBC surface (Figure 1C). Human TIM-4-Ig, hTIM-1-Ig, mTIM-4(IgV)-Ig, and mTIM-1(IgV)-Ig did not bind detectably to fresh RBCs but bound strongly to eryptotic RBCs (Figure 1D and data not shown). In contrast, mTIM-2(IgV)-Ig or control Ig did not bind to any cell tested. Similar binding results with these TIM-Ig were seen with several mouse (300.19, FL5.12) and human (Jurkat, U937) cell lines after induction of apoptosis by various methods (cytokine deprivation, etoposide, Fas-mediated) (data not shown). Binding was not species restricted. In contrast, freshly isolated human T cells did not bind any of the TIM-Ig (data not shown).

By preincubating TIM-Ig with TIM mAbs known to recognize the IgV domain, we tested the capacity of TIM mAbs to block the interaction with apoptotic cells. The interaction of hTIM-4-Ig with apoptotic cells was blocked by hTIM-4 mAb 9F4 but not by mAb 4E11 (Figure 1E). The interaction of hTIM-1-Ig was blocked by hTIM-1 mAb 3D1 and moderately blocked by hTIM-1 mAb 1D12 (Figure 1F). Thus, blockade by mAbs that recognize the IgV domain as well as binding by TIM-4 and TIM-1 fusion proteins containing the IgV but not the mucin domain indicates that the critical recognition structure for apoptotic cells is contained in the IgV domain alone.

### TIM-4 and TIM-1 Bind to PS

Exposure of PS on the outer-membrane leaflet is a major difference between live and apoptotic cells, so we tested whether TIM-1 and TIM-4 recognize PS by using PS-coated plates in a solid-phase enzyme-linked immunosorbent assay (ELISA). Murine TIM-1(IgV)-Ig and mTIM-4(IgV)-Ig bound to PS-coated plates in a concentration-dependent manner; however, mTIM-2(IgV)-Ig did not bind (Figure 2A). Human TIM-1-Ig, hTIM-4-Ig, mTIM-1(IgV)-Ig, and mTIM-4(IgV)-Ig bound to plates coated with PS, but not to plates coated with phosphatidylinositol (PI), phosphatidylcholine (PC), or phosphatidylethanolamine (PE) (Figure 2B). Murine TIM-2(IgV)-Ig did not bind to any of these phospholipids, even at high concentrations of TIM-2-Ig.

To determine the binding of TIM proteins to other phospholipids, we employed a protein-lipid overlay assay using nitrocellulose membranes on which various phospholipids had been spotted (PIP strip). Figure 2C shows that mTIM-1 and mTIM-4 specifically bound to PS but not to the other phospholipids, except for a slight binding to cardiolipin. These findings indicate that human and mouse TIM-1 and TIM-4 specifically recognize PS via the IgV domain of the TIM molecule.

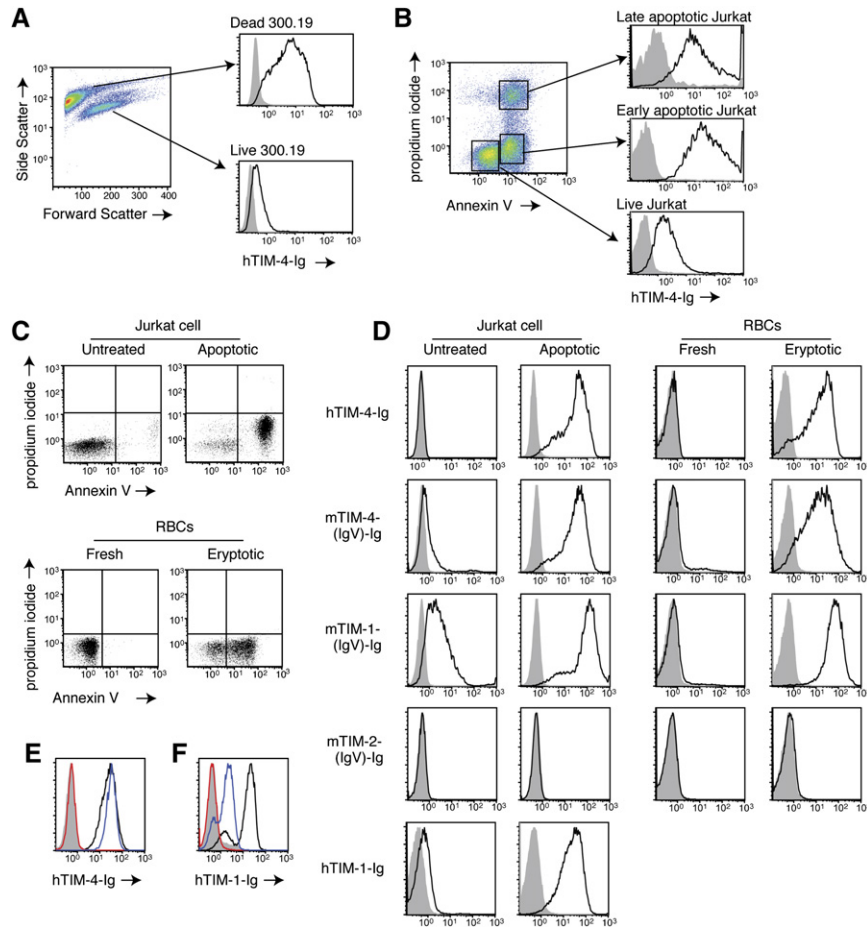


**Figure 1. TIM-4 and TIM-1, but Not TIM-2, Fusion Proteins Bind to Apoptotic Cells**

(A) An overgrown culture of 300.19 cells was stained with hTIM-4-Ig (open curves) or control mIgG2a (filled gray curves). Cells gated on live or dead cells by forward and side scatter were analyzed by flow cytometry. Data shown are representative of more than five experiments.

(B) Jurkat cells treated with Fas mAb were stained with hTIM-4-Ig (open curves) or control mIgG2a (filled gray curves) followed by allophycocyanin-conjugated goat anti-mouse IgG2a and annexin-V FITC and propidium iodide. Cells gated on live, early, and late apoptotic cells as indicated were analyzed by flow cytometry. Data shown are representative of more than five experiments.

(C) Jurkat cells untreated (left panel) or made apoptotic with Fas mAb (right panel) were ficollized to remove late apoptotic cells and stained with annexin-V FITC and propidium iodide. Fresh untreated RBCs (left panel) or RBCs made eryptotic by treatment with ionomycin and  $\text{CaCl}_2$  (right panel) were stained with annexin-V FITC and propidium iodide. Data shown are representative of three experiments.

(D) Untreated or apoptotic Jurkat cells and fresh or eryptotic RBCs made as in (C) were stained with 1.2  $\mu\text{g}/\text{ml}$  of hTIM-4-Ig, or with 5  $\mu\text{g}/\text{ml}$  of mTIM-1(IgV)-Ig, mTIM-2(IgV)-Ig, or mTIM-4(IgV)-Ig (open curves), or with isotype control mouse IgG2a (filled gray curves). Ig FPs were detected with PE-conjugated anti-mouse IgG2a. Live or apoptotic Jurkat cells were stained with hTIM-1-Ig or isotype control and detected with PE-conjugated anti-human IgG. Data shown are representative of three or more experiments.

(E) Human TIM-4-Ig was preincubated with 10  $\mu\text{g}/\text{ml}$  of TIM-4 mAbs 9F4 (red line), 4E11 (blue line), or isotype control mouse IgG1 (black line) before the staining of apoptotic Jurkat cells. Filled gray indicates the staining with isotype control mouse IgG2a. Data are representative of three experiments.

(F) Human TIM-1-Ig was preincubated with 10  $\mu\text{g}/\text{ml}$  of TIM-1 mAbs 3D1 (red line), 1D12 (blue line), or isotype control (black line) before the staining of apoptotic Jurkat cells. Filled gray indicates staining with control hIgG FP. Data shown are representative of three experiments.

### Human TIM-1 and TIM-4 Facilitate Engulfment of Apoptotic Cells by Transfected NIH 3T3 Cells

Recognition of cell-surface PS is a critical signal for clearance of dead cells by phagocytes (Fadok et al., 1992; Verhoven et al., 1995). To study the function of TIM-1 and TIM-4 in phagocytosis of apoptotic cells, we transfected hTIM-1 or hTIM-4 into NIH 3T3 cells. Stable hTIM-1 or hTIM-4-3T3 expressed moderate amounts of

each molecule on their cell surfaces (Figure S1 available online). Flow cytometry was used to measure uptake of CMTMR-labeled live or apoptotic U937 cells or PKH67-labeled fresh or eryptotic RBCs by transfected 3T3 cells (Figures 3A–3C). Live U937 cells or fresh RBCs did not bind and were not phagocytosed by TIM-1, TIM-4, or untransfected 3T3 cells. In contrast, apoptotic U937 (Figures 3A and 3B) or eryptotic RBCs (Figure 3C) were rapidly

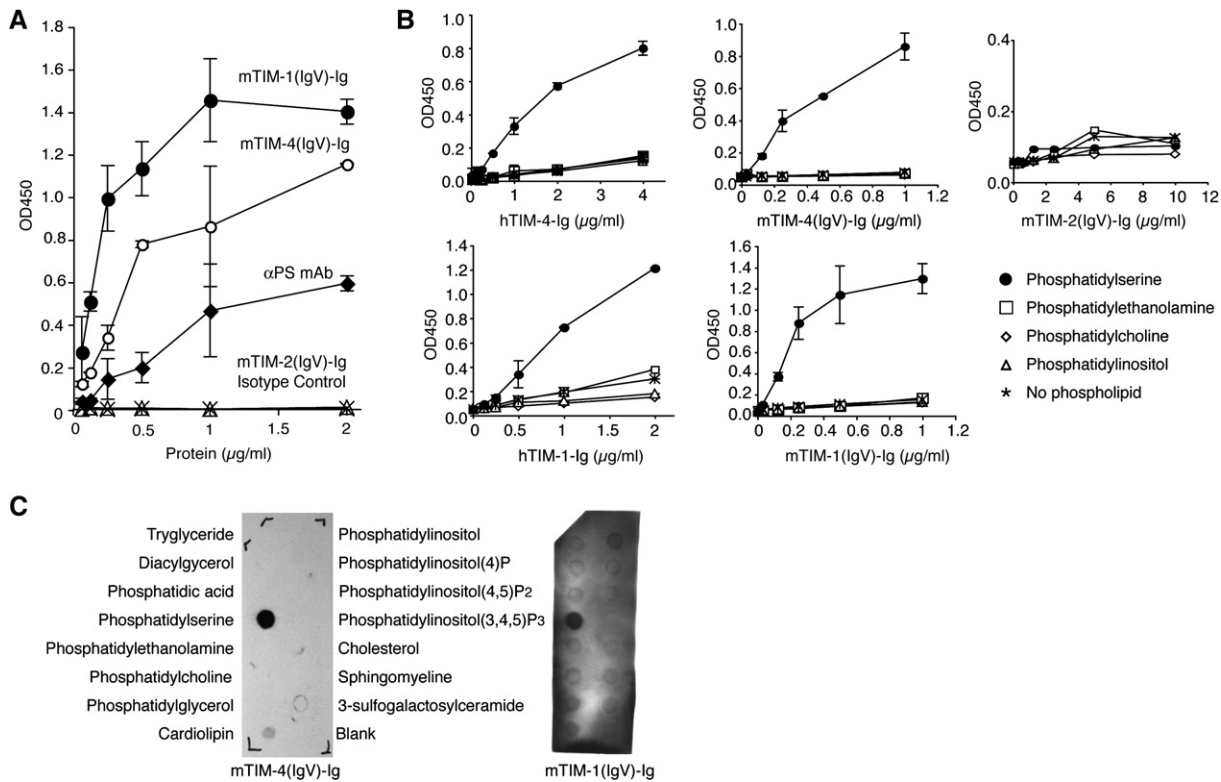


**Figure 2. TIM-1 and TIM-4, but Not TIM-2, Bind to Phosphatidylserine and Not Other Phospholipids**

(A) ELISA plates coated with PS were incubated with mTIM-4(lgV)-Ig, mTIM-1(lgV)-Ig, mTIM-2 (lgV)-Ig, anti-PS mAb, or isotype control mouse IgG2a as indicated. Fusion proteins not bound to the plates were removed by washing, and bound protein was quantified by ELISA. Data are shown as mean  $\pm$  standard deviation (SD) of duplicate wells and are representative of three independent experiments.

(B) ELISA plates coated with PS, PE, PC, or PI or without phospholipid were incubated with the indicated concentrations of hTIM-4-Ig, hTIM-1-Ig, mTIM-4(lgV)-Ig, mTIM-1(lgV)-Ig, or mTIM-2(lgV)-Ig. TIM-Ig bound to wells was quantified by ELISA. Data are shown as mean  $\pm$  SD of duplicate wells and are representative of three independent experiments.

(C) mTIM-4 and mTIM-1 bind strongly to phosphatidylserine on PIP strips. Two micrograms per milliliter of mTIM-4(lgV)-Ig (left) or mTIM-1(lgV)-Ig (right) were incubated with strips spotted with the indicated phospholipids, washed, and developed with anti-mouse IgG2a-HRP. Data shown are representative of two experiments.

and efficiently phagocytosed by hTIM-1- or hTIM-4-transfected 3T3. Apoptotic U937 or eryptotic RBCs were slowly and inefficiently phagocytosed by untransfected 3T3. Electron microscopy and three-dimensional imaging by confocal microscopy showed that uptake of apoptotic U937 by TIM-1- or TIM-4-transfected cells was truly phagocytosis because the apoptotic cells were completely engulfed and internalized (Figures 3D–3I and data not shown). Labeling of apoptotic U937 with the pH-sensitive dye, CypHer5E (Beletskii et al., 2005), showed that the phagocytosed U937 was compartmentalized into an acidic compartment such as a phagosome (Figure 3E and Figure S5). Using eryptotic RBCs, we saw a similar enhancement of phagocytosis in TIM-1- or TIM-4-transfected 3T3 cells. (Figure S2).

To test whether PS is the molecule recognized by TIM-1 and TIM-4 in phagocytosis of apoptotic cells, we prepared phospholipid liposomes containing various phospholipids and tested their capacity to inhibit phagocytosis by TIM transfected cells. Liposomes containing equal amounts of PS and PC (PS + PC) reduced phagocytosis by both

TIM-1 and TIM-4 transfectants in a concentration-dependent fashion with complete inhibition at 10  $\mu$ M of total phospholipids (Figure 3J). Inhibition of phagocytosis was not observed with liposomes containing another anionic lipid, PI, nor with PC or PE (Figures 3J and 3K). These observations show that recognition of PS on the plasma membrane by hTIM-4 and hTIM-1 depends not only on the anionic charge of PS but also on highly specific recognition of PS structural features.

#### TIM-4 Is Expressed by Macrophages and Dendritic Cells

TIM-4 mRNA expression has been reported in mouse spleen and lymph node (Meyers et al., 2005; Shakhov et al., 2004), but which cells display surface TIM-4 is unclear. We found that resident mouse peritoneal cells express higher amounts of TIM-4 mRNA than splenocytes (Figure 4A). To identify the cell-surface expression of TIM-4, we used two-color staining with F4/80 to identify peritoneal macrophages (PM $\phi$ ) and either of two mTIM-4 mAbs. PM $\phi$  expressed high amounts of TIM-4 but no

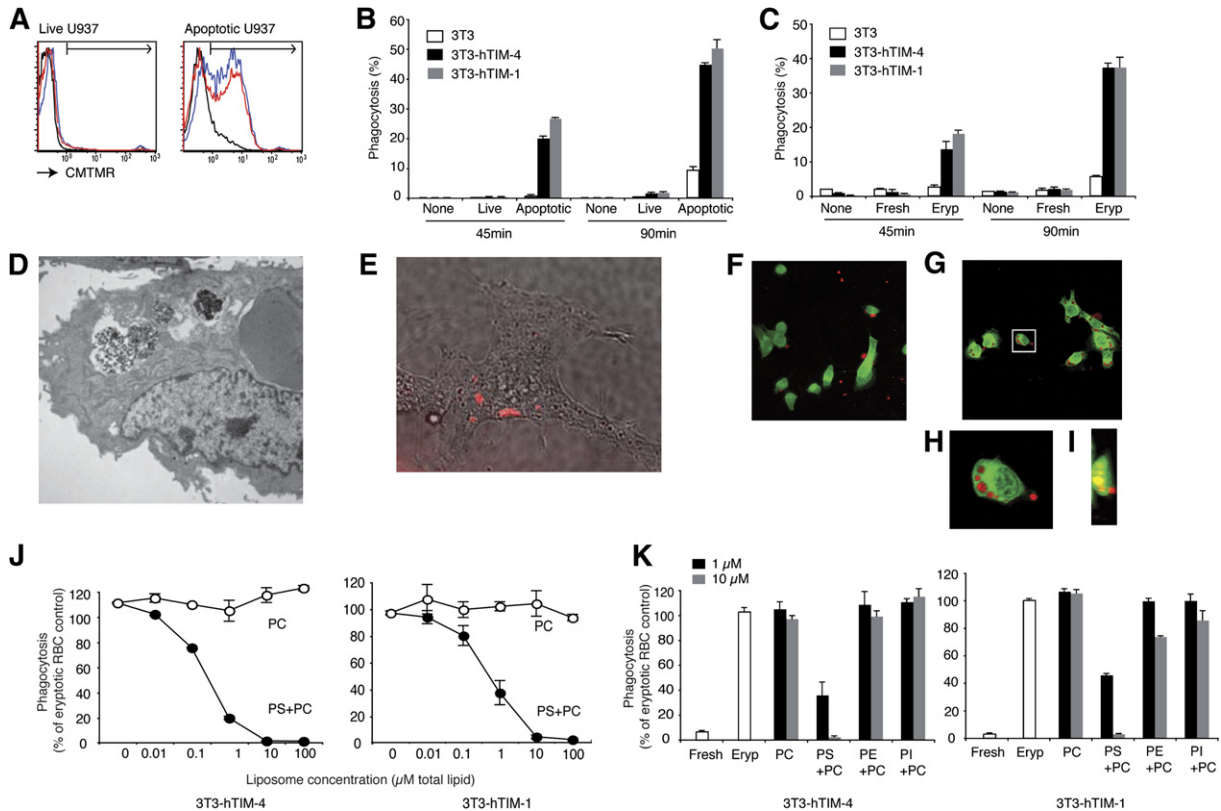


**Figure 3. hTIM-1- or hTIM-4-Transfected NIH 3T3 Cells Phagocytose Apoptotic U937 Cells or Eryptotic RBCs but Not Live Cells**

(A–D) CMTMR-labeled live or apoptotic U937 or PKH67-labeled live or eryptotic (Eryp) RBCs were cocultured with 3T3, hTIM-1 3T3, or hTIM-4 3T3 for 45 or 90 min, nonadherent cells were washed off, and adherent cells were detached and analyzed by flow cytometry or electron microscopy for phagocytosis of labeled cells. (A) FACS profiles for phagocytosis of live or apoptotic U937 by 3T3 (black line), hTIM-1 3T3 (blue line), or hTIM-4 3T3 (red line) after 90 min cocubation. Data are representative of three experiments. (B and C) Phagocytosis assays with (B) U937 cells or (C) RBCs were done in duplicate, and mean values are plotted with SD and are representative of three experiments. (D) Electron micrograph of apoptotic U937 phagocytosed by hTIM-4 3T3. Original magnification was 5000 $\times$ . Data are representative of two experiments.

(E) Photomicrograph of CypHer5E-labeled apoptotic U937 compartmentalized to an acidic compartment of hTIM-4 3T3. Data are representative of two experiments.

(F–I) 3T3 cells (F) or hTIM-1 3T3 (G–I) were labeled with CMFDA (green). U937 were labeled with CMTMR (red) and made apoptotic by 5 hr treatment with etoposide. 3T3 cells and apoptotic U937 cells were cocultured for 2 hr, washed, and visualized by confocal microscopy as described in the [Experimental Procedures](#). An enlarged image of the boxed region in (G) is shown in (H), and a side image is shown in (I). Data are representative of two experiments.

(J) Phagocytosis of eryptotic RBCs by hTIM-1 3T3 or hTIM-4 3T3 was inhibited by liposomes containing a 50:50 mix of PS and PC but not by PC alone. hTIM-1 or TIM-4 3T3 were preincubated with liposomes for 15 min and cocultured with PKH67-labeled eryptotic RBCs for 45 min. After the washing out of nonattached cells, 3T3 cells were detached and analyzed by flow cytometry for phagocytosis of eryptotic RBCs. Phagocytosis of eryptotic RBCs in the absence of liposomes represents 100%. Data are shown as mean  $\pm$  SD of duplicate wells and are representative of three independent experiments.

(K) Phagocytosis of eryptotic RBCs by hTIM-1 or hTIM-4 3T3 was inhibited by liposomes containing PS but not PC, PE, or PI. hTIM-1 or TIM-4 3T3 cells were preincubated with 1 or 10  $\mu$ M of liposomes containing the indicated phospholipids. Assays were done as described in (J). Data are shown as mean  $\pm$  SD of duplicate wells and are representative of three independent experiments.

detectable TIM-1 (Figure 4B). TIM-4 staining was present in moderate abundance on both CD8 $\alpha^+$  and CD8 $\alpha^-$  subsets of CD11c $^+$  DCs, consistent with the initial identification of TIM-4 mRNA expression in CD11c $^+$  cells (Meyers et al., 2005), but was not detectable on plasmacytoid DCs (Figure 4C) or GM-CSF-stimulated bone-marrow-derived DCs (data not shown). TIM-4 was not detected on unstimulated CD19 $^+$  B cells (Figure 4C) or B cells stimulated with lipopolysaccharide (LPS) or CD40 mAb (data

not shown). TIM-4 was not detected on resting or activated T cells, but TIM-1 was expressed on activated T cells (Umetsu et al., [2005] and data not shown).

Human lymphoid tissues such as tonsil, thymus, and spleen, as well as testis, expressed TIM-4 mRNA by qRT-PCR (Figure 4D). Kidney, liver, and lung expressed low amounts of TIM-4 mRNA, and peripheral blood mononuclear cells (PBMCs) expressed very low amounts. To determine whether human M $\phi$  express TIM-4, we

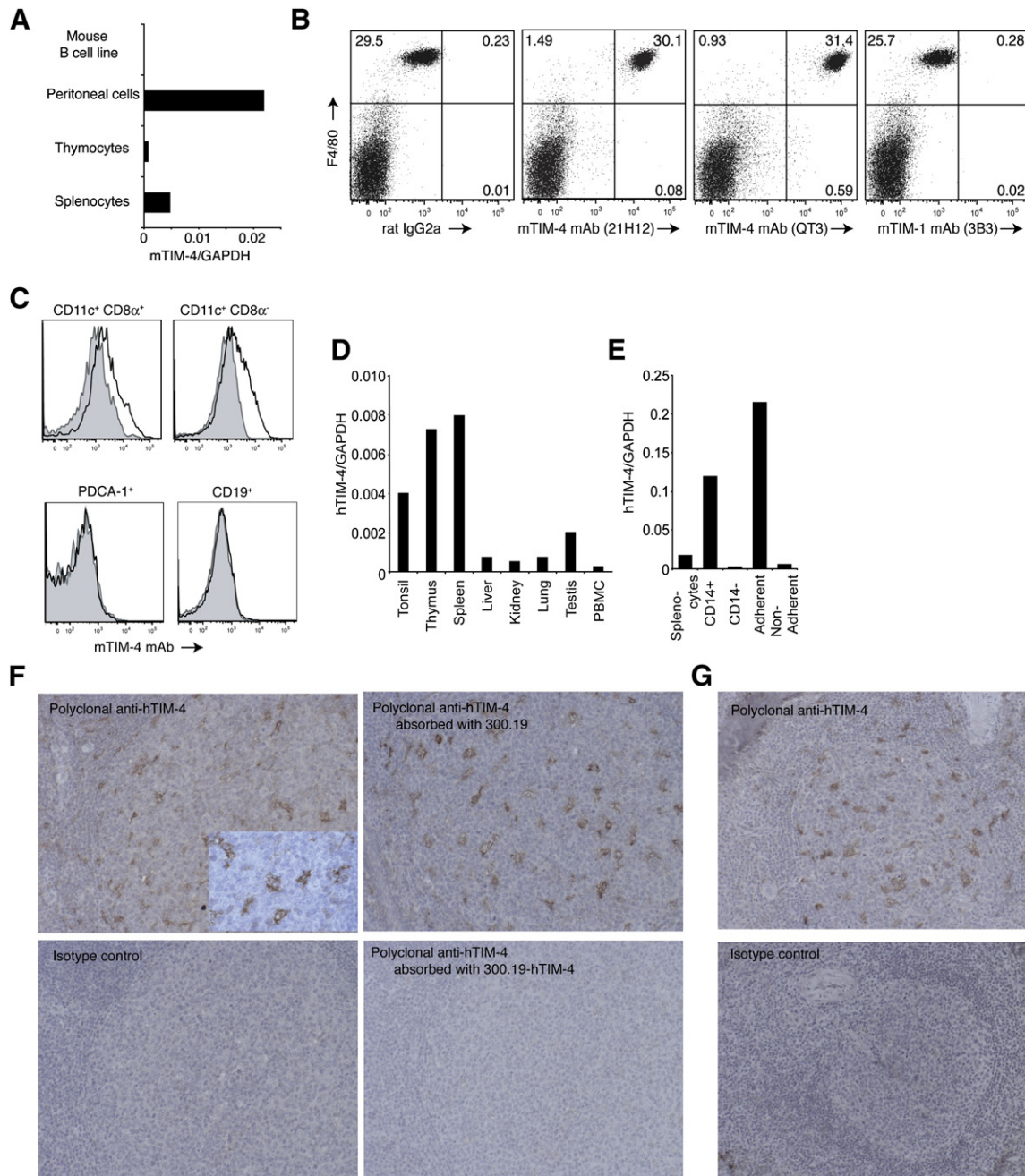


**Figure 4. TIM-4 Is Expressed in Macrophages and Dendritic Cells**

(A) qRT-PCR analysis of TIM-4 mRNA expression in the indicated mouse tissues and a mouse pre-B cell line (300.19). Data are representative of three experiments.

(B) Cell-surface expression of mTIM-4. Mouse resident peritoneal cells were stained with F4/80-allophycocyanin mAb and anti-mTIM-4-PE mAb (21H12 or QT3) or anti-mTIM-1-PE and analyzed by flow cytometry. The percent of cells in each quadrant is indicated. Data are representative of four experiments.

(C) Mouse splenic cells were stained with the indicated lineage-specific markers and anti-mTIM-4-PE. Filled gray curves represent isotype-control staining, and open curves represent staining of lineage-gated cells with mTIM-4 mAb. Results are representative of three experiments.

(D) qRT-PCR analysis of TIM-4 mRNA expression in the indicated human tissues. Data are representative of two experiments.

(E) qRT-PCR analysis of TIM-4 mRNA expression in human splenic macrophages. Splenic macrophages were enriched with CD14 MACS beads or by adhesion as described in *Experimental Procedures*. Data are representative of three experiments.

(F–G) Immunohistochemistry showing TIM-4 expression in (F) human tonsil and (G) spleen. Sections of paraffin-embedded tissue were stained with polyclonal hTIM-4 antibody. Isotype control was normal goat IgG. All micrographs were obtained with the 20 $\times$  objective, except for the inserted frame in the upper-left panel in (F) (40 $\times$ ). Staining is representative of five or more experiments except for absorbed antisera, which was done once.

prepared human splenic M $\phi$  either by positive selection with CD14 MACS microbeads or by adherence to tissue-culture plastic (see [Experimental Procedures](#)). Splenic adherent and CD14<sup>+</sup> cells expressed high amounts of TIM-4 mRNA, whereas nonadherent and CD14<sup>-</sup> cells expressed little TIM-4 mRNA ([Figure 4E](#)). Human splenic CD14<sup>high</sup>CD11c<sup>low</sup>CD11b<sup>+</sup> cells, consisting of M $\phi$  and immature DCs, expressed high amounts of TIM-4 mRNA, but CD14<sup>-</sup>CD11c<sup>high</sup>CD11b<sup>-</sup>, consisting of mature DCs in human spleen, expressed little TIM-4 mRNA (data not shown). Human peripheral blood monocytes did not express detectable amounts of cell-surface TIM-4 (data not shown).

To further characterize the expression of TIM-4 in human tissue, we performed immunohistochemistry of tonsil ([Figure 4F](#)) and spleen ([Figure 4G](#)) with goat anti-hTIM-4 polyclonal antibody. Tingible-body M $\phi$  located in germinal centers of tonsil or white pulp of spleen showed expression for TIM-4. Tingible bodies are the remnants of cells phagocytosed by macrophages, and tingible-body macrophages are the cells that engulf apoptotic cells in lymphoid tissue ([Smith et al., 1991](#)). There was no staining with control goat IgG ([Figures 4F and 4G](#)). The specificity of TIM-4 staining was further confirmed by showing that absorption of the TIM-4 antibody on TIM-4 transfected 300.19 cells removed the reactivity, whereas absorption on untransfected 300.19 cells did not ([Figure 4F](#)). These results show that macrophages in human and mouse express TIM-4.

#### Phagocytosis of Apoptotic Thymocytes by Mouse Peritoneal Macrophages Was Reduced by TIM-4 mAb

To assess the involvement of TIM-4 in phagocytosis of apoptotic cells, we preincubated PM $\phi$  with increasing amounts of 21H12 mAb or isotype control. PM $\phi$  were then cocultured with PKH67-labeled apoptotic thymocytes for 30 min, and phagocytosis was measured by flow cytometry ([Figures 5A and 5B](#)). Approximately 44% of the PM $\phi$  phagocytosed apoptotic thymocytes, and this percentage was not affected by isotype control antibody. In contrast, 2 or 10  $\mu$ g/ml of mTIM-4 mAb 21H12 reduced the percentage of PM $\phi$  that engulfed apoptotic cells to 13.6%. These results suggested that TIM-4 is one of the receptors used by mouse PM $\phi$  to recognize and phagocytose apoptotic cells.

#### The Human Kidney Cell Line 769P Phagocytoses Apoptotic Cells through Human TIM-1

Some human kidney cell lines show natural surface expression of TIM-1. We confirmed that 769P cells ([Vila et al., 2004](#)), derived from a renal clear-cell carcinoma, express TIM-1 on their cell surface by using hTIM-1 antibody 3D1 ([Figure 6A](#)). In contrast, 769P cells did not express TIM-4. To test whether 769P cells phagocytose apoptotic cells via TIM-1, we cultured 769P cells with apoptotic U937 cells or eryptotic RBCs and measured phagocytosis. During a 2 hr incubation, 769P cells phagocytosed apoptotic U937 (41.9%), but not live U937 (0.35%) (data

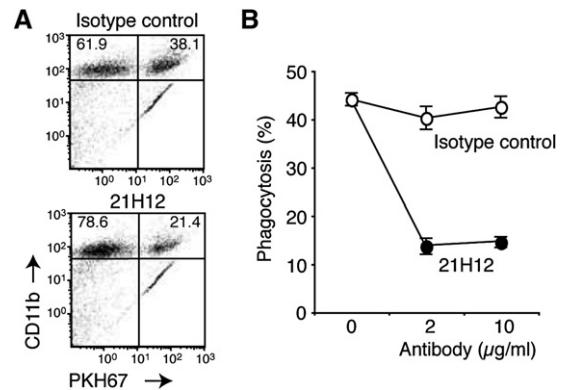


**Figure 5. TIM-4 mAb Blocked Phagocytosis of Apoptotic Thymocytes by Mouse Peritoneal Macrophages**

(A) Mouse PM $\phi$  were preincubated with 10  $\mu$ g/ml isotype control or 21H12 mTIM4 mAb for 5 min followed by PKH67-labeled apoptotic thymocytes for 30 min. Nonadherent cells were removed by washing, and PM $\phi$  were detached and stained with anti-CD11b-PE. The phagocytosis of PKH67-labeled apoptotic thymocytes by CD11b<sup>+</sup> cells was analyzed by flow cytometry, and the percent of cells in each quadrant is indicated. Data are representative of four experiments.

(B) Phagocytosis assays were performed as in (A) with the indicated concentrations of 21H12 or isotype control. Data are shown as mean  $\pm$  SD of duplicate wells and are representative of three independent experiments.

not shown). The internalization of apoptotic cells was confirmed by three-dimensional imaging by confocal microscopy ([Figure 6B](#)). 769P cells also phagocytosed eryptotic RBCs much more efficiently than fresh RBCs ([Figure 6C](#)). Using the TIM-1 mAbs 3D1 and 1D12, which blocked the binding of TIM-1-Ig to apoptotic Jurkat cells ([Figure 1F](#)), we found that binding and phagocytosis of apoptotic cells was blocked by these TIM-1 antibodies in a concentration-dependent manner ([Figure 6D](#) and [Figure S3](#)). These studies show that 769P cells can recognize and phagocytose apoptotic cells through TIM-1 on their cell surface.

#### CC'FG Ligand Binding Cavity Is Critical for Phagocytosis of Apoptotic Cells

The crystal structure of mTIM-4 showed that PS binds in the cavity built up by the CC' and FG loops and suggests that this cavity is important for biological function ([Santiago et al., 2007a](#)). To test the function of this site in phagocytosis of apoptotic cells, we prepared alanine substitutions of each of the four amino acids comprising this cavity at the FG loop (W119-D122). Hydrophobic W119 and F120 are located at the top of the FG loop. N121 and D122 are at the bottom of this cavity and trap positively charged ions. Each mutant was transfected into NIH 3T3 cells, and transfectants were identified with polyclonal goat anti-hTIM-4 antibody ([Figure 7A](#)). Alanine substitutions in W119-D122 did not affect binding by the 4E11 hTIM-4 mAb. In contrast, the W119A, F120A, or N121A—but not D122A—substitution destroyed the epitope that is on TIM-4 and recognized by the 9F4 mAb. These results show that 9F4 mAb recognizes the FG

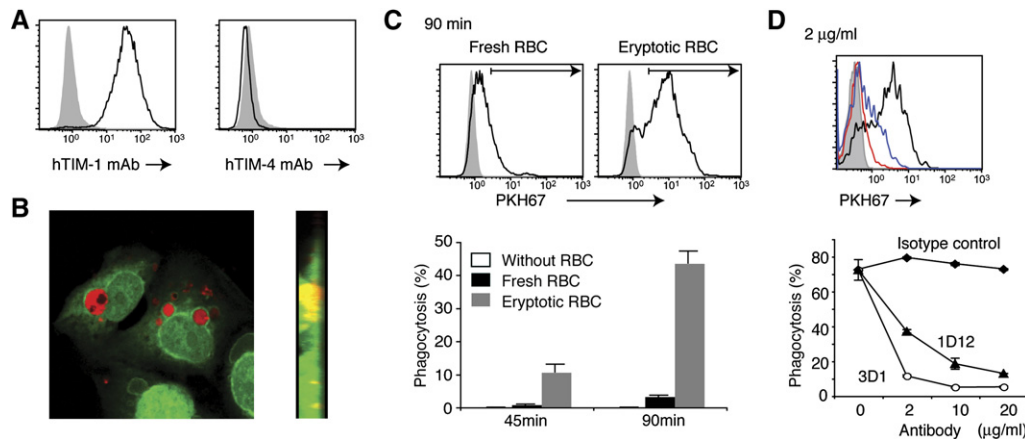


**Figure 6. Human Kidney Cell Line 769P Expressed hTIM-1 and Phagocytosed Apoptotic U937 Cells and Eryptotic RBCs through hTIM-1**

(A) 769P cells were stained with PE-conjugated hTIM-1 mAb (3D1) or hTIM-4 mAb (9F4) (open curves) or isotype control (filled gray curves) and analyzed by flow cytometry. Data are representative of three experiments.

(B) CMFDA-labeled 769P cells (green) and CMTMR-labeled apoptotic U937 cells (red) were cocultured for 2 hr, nonadherent cells were washed off, and remaining cells were fixed and visualized by confocal microscopy. The right panel shows a side view of the left panel. Data are representative of two experiments.

(C) PKH67-labeled fresh and eryptotic RBCs were cocultured with 769P cells for 45 min or 90 min, nonadherent cells were washed off, and remaining cells were detached and analyzed for PKH67-positive RBCs in 769P cells by flow cytometry. The FACS profiles for PKH67-positive RBCs in 769P cells (open curves) and 769P cells without RBCs (filled gray curves) are shown in the upper panel and presented graphically in the lower panel. Assays were done in duplicate, and mean values are plotted with SD. Data are representative of four experiments.

(D) Phagocytosis of eryptotic RBCs was blocked by hTIM-1 mAb. 769P cells were preincubated with 3D1, 1D12, or isotype control for 30 min and cocultured with PKH67-labeled eryptotic RBCs for 90 min; nonadherent cells were washed off, and remaining cells were detached and analyzed for PKH67-positive RBCs in 769P by flow cytometry. FACS profiles for PKH67-positive RBCs in 769P incubated with 2  $\mu$ g/ml 3D1 (red line), 1D12 (blue line), or isotype control (black line) are shown in the upper panel and presented graphically in the lower panel. Filled gray curve represents 769P cells in the absence of RBCs. Data are shown as mean  $\pm$  SD of duplicate wells and are representative of three independent experiments.

loop of hTIM-4, whereas the 4E11 mAb reacts outside this area. This epitope mapping is consistent with the capacity of 9F4, but not 4E11, to reduce phagocytosis of eryptotic RBCs by hTIM-4 transfected 3T3 cells (Figure 7B).

The phagocytic capacity of untransfected, wild-type, and mutant TIM-4-transfected 3T3 cells was compared (Figures 7C and 7D and Figure S4). Wild-type hTIM-4-transfected 3T3 efficiently phagocytosed eryptotic RBCs with 70% of the cells phagocytosing an RBC after 90 min, whereas untransfected 3T3 phagocytosed eryptotic RBCs poorly, with only 17% of the cells phagocytosing an RBC after 90 min. All 3T3 lines transfected with mutant TIM-4 (W119A, F120A, N121A, and D122A) had reduced phagocytic activity equivalent to that of untransfected 3T3. These results show that the PS binding cavity composed of W119 to D122 is necessary for the recognition and phagocytosis of apoptotic cells by TIM-4.

## DISCUSSION

In this study we have shown that TIM-4 and TIM-1 recognize PS on the surface of apoptotic cells. TIM-4 mAb reduced phagocytosis of apoptotic cells by PM $\phi$ . Transfection of TIM-4 or TIM-1 into NIH 3T3 cells greatly augmented their capacity to phagocytose apoptotic cells. This phagocytic activity was completely blocked by liposomes containing PS but not PC, PI, or PE. We identified

mAbs that were against mouse and human TIM-4 and TIM-1 and would block binding to PS and phagocytosis. All the blocking mAbs mapped to the IgV domain on which the PS binding cavity is located. Consistent with a role in recognition of apoptotic cells, TIM-4 is highly expressed on phagocytic cells such as peritoneal macrophages, tinged-body macrophages, and dendritic cells.

PS comprises about 7% of the phospholipid of a cell but is compartmentalized to the inner leaflet of the cell membrane. The redistribution of PS to the external surface of the plasma membrane is a key element of apoptotic cell recognition and is a molecular cue that dying cells should be phagocytosed (Fadok et al., 1992; Verhoven et al., 1995). Healthy Jurkat cells expose about 0.9 attomol (600,000 molecules) of PS per cell, which rises to about 240 attomol/cell late in apoptosis (Borisenko et al., 2003). Macrophages inefficiently phagocytose Jurkat cells expressing this low, healthy level of PS, and phagocytosis increases only after a threshold surface level of about 5 attomol/cell is passed and plateaus above 25 attomol/cell (Borisenko et al., 2003). All healthy long-term cell lines showed a low amount of binding of TIM-1 and TIM-4, consistent with their low but detectable exposure of cell-surface PS as measured by PS mAb or AnnexinV-FITC (data not shown). In contrast, TIM-1 and TIM-4 did not bind to T cells from freshly isolated blood (data not shown). This is consistent with the fact that in vivo,



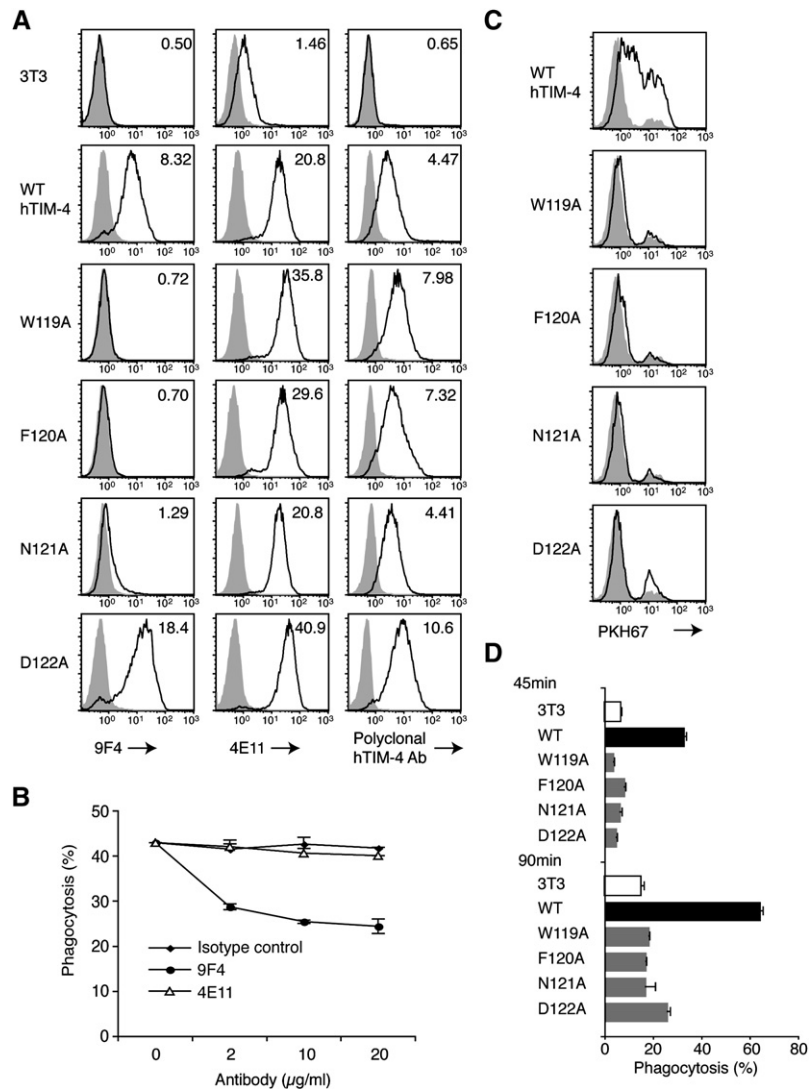


**Figure 7. Mutants in the hTIM-4 CC/FG Cavity Do Not Phagocytose Apoptotic Cells**

(A) Binding of hTIM-4 antibodies to mutant hTIM-4-transfected 3T3 cell lines. Wild-type hTIM-4 and mutant hTIM-4 (W119A, F120A, N121A, and D122A) were transfected into NIH 3T3 cells. Wild-type or mutant hTIM-4 3T3 were stained with 9F4, 4E11, or polyclonal hTIM-4 antibody and analyzed by flow cytometry. Open curves represent staining with hTIM-4 antibody, and the filled gray curves represent staining with isotype control antibody. Numbers in the panels are mean fluorescence intensity of the TIM-4-stained cells. Data are representative of two experiments.

(B) 9F4 but not 4E11 blocked phagocytosis of eryptotic RBCs by hTIM-4 3T3. hTIM-4 3T3 were preincubated with 9F4, 4E11, or isotype control mouse IgG1 for 30 min and cocultured with PKH67-labeled eryptotic RBCs; nonadherent cells washed off, and remaining cells were detached and analyzed for PKH67-positive RBCs in hTIM-4 3T3 by flow cytometry. Assays were done in duplicate, and mean values are plotted with SD. Data are representative of three experiments.

(C and D) Phagocytosis of PKH67-labeled eryptotic RBCs by mutant TIM-4 3T3. The indicated TIM-4 3T3 transfectants were cocultured with PKH67-labeled eryptotic RBCs, nonadherent cells were washed off, and remaining cells were detached and analyzed for PKH67-positive RBCs in hTIM-4 3T3 by flow cytometry. FACS profiles of 90 min culture are shown in (C). Filled gray curves represent untransfected 3T3 with eryptotic RBCs, and open curves represent the indicated TIM-4 transfectant with eryptotic RBCs. Results at 45 and 90 min are presented graphically in (D). Data are shown as mean  $\pm$  SD of duplicate wells and are representative of three independent experiments.

cells exposing PS are rapidly phagocytosed, whereas in vitro, cell lines are not monitored as stringently because professional phagocytic cells are not present.

Several receptor combinations that participate in the recognition of PS on the surface of apoptotic cells have been identified, including Milk fat globule EGF-factor 8 (MFG-E8) (Hanayama et al., 2002) and Growth arrest-

specific gene 6 (GAS6) (Scott et al., 2001). These are two component systems composed of a soluble PS “tethering” molecule such as MFG-E8 or GAS6 and a membrane-bound “tickle” molecule, such as  $\alpha_V\beta_3$  or  $\alpha_V\beta_5$  integrin or Mer, responsible for recognition of the “tether” and internalization and signaling. A PS receptor on the surface of macrophages has been described; however, the

candidate molecule cloned by phage display (Fadok et al., 2000) has been discredited (Williamson and Schlegel, 2004). TIM-4 is a likely candidate for this macrophage PS receptor, with the IgV domain forming the “tether” that binds PS and the extended mucin domain providing a “tickle” to the TIM transmembrane and cytoplasmic domains. Although the involvement of TIM-4 in phagocytosis seems clear, the cytoplasmic domain of TIM-4 does not contain any tyrosine signaling motifs, and the signaling pathway requires further study. Recognition of PS by TIM-4 and TIM-1 was highly specific, whereas other PS-binding molecules such as MFG-E8 (Hanayama et al., 2002), GAS6 (Nagata et al., 1996; Nakano et al., 1997),  $\beta$ 2-glycoprotein (Balasubramanian et al., 1997), and lectin-like oxidized low-density lipoprotein receptor 1 (Oka et al., 1998) bind not only PS but also other anionic phospholipids.

Phagocytosis of apoptotic cells is evolutionarily ancient, and PS-recognition molecules such as MFG-E8 and GAS6 are broadly expressed in tissues. In contrast, expression of TIM-4 is highly restricted to professional antigen-presenting cells (APCs) and testis, suggesting an immunologically restricted function in recognition of apoptotic cells. Given the redundant systems that recognize apoptotic cells, the strong effects of TIM-1 or TIM-4 mAbs or fusion proteins are impressive.

The cocrystal structure of PS bound to TIM-4 shows a direct interaction not mediated by intervening molecules (Santiago et al., 2007a). The specific binding of PS to TIM-4 is due to the unique structure of TIM IgV domains. The four noncanonical cysteines found in all TIM family members form disulfide bonds that reverse and fix the folded conformation of the long CC' loop onto the GFC  $\beta$  sheet (Cao et al., 2007; Santiago et al., 2007b). Instead of the relatively flat binding surface found in most Ig superfamily ligand-recognition surfaces, the CC'FG loops form a narrow cavity with dimensions of approximately  $7 \times 9 \times 11 \text{ \AA}$ . The outer lips of the cavity are composed of hydrophobic amino acids positioned to interact with the hydrophobic fatty-acid region of PS. The bottom of the cavity is composed of charged amino acids that capture a metal ion and coordinate with the charged head of the PS.

Mutation of any of the amino acids (119–122, WFND) that line this binding cavity eliminates binding to PS and phagocytosis. The 9F4 mAb that blocks TIM-4 binding to PS maps to this epitope. The structures of mouse and human TIM-1 and TIM-4 are very highly conserved in this region, whereas TIM-2 is completely different (–AF, where – indicates a gap in the aligned sequences). This probably explains the similar recognition of PS by TIM-4 and TIM-1 and the different ligand binding of TIM-2. Clearly, TIM-2 is an outlier in the TIM family, and binding to proteins including Semaphorin4A and h-Ferritin has been reported. TIM-1 and TIM-4 have been reported to be ligands for each other on the basis of the binding of TIM-1-Ig to TIM-4 transfectants and vice versa (Meyers et al., 2005); however, Biacore studies with highly purified protein showed the TIM-1:TIM-4 interaction was of very

low affinity (Sizing et al., 2007). In our assays of TIM-mediated phagocytosis, the apoptotic cell did not express TIM-1 or TIM-4, thereby excluding a TIM:TIM interaction. Some of the low-level, universal binding of TIM proteins observed by us and others (Cao et al., 2007; Wilker et al., 2007) might reflect the health of the cell and its level of exposure of PS. In addition, some apparent TIM-1:TIM-4 interactions could reflect a “bridge” with two TIM proteins binding to a membrane fragment via exposed PS.

TIM-1 was also cloned as kidney injury molecule 1 (KIM-1) and is expressed minimally by healthy kidney but in postischemic kidney is highly unregulated on the luminal side of dedifferentiated tubule epithelial cells (Ichimura et al., 1998). Although the function of TIM-1 in recovery from ischemic-kidney injury is not yet clear, our results show that TIM-1 on a renal cell carcinoma line mediates phagocytosis of apoptotic cells and suggests that one of the functions of TIM-1 on dedifferentiated tubular epithelial cells might be recognition of dead cells after ischemic-kidney injury and clearance of dead cells to reconstitute the tissue. In addition, TIM-1 ectodomain has been shown to be shed from the injured kidney (Han et al., 2002) and may regulate the recognition of apoptotic cells either by opsonization or by blockade. Although TIM-1 can mediate phagocytosis in a large kidney cell, it may function on a small T cell more to receive signals via small exosomes or to sense the activation status of the T cell and the health of the APC and surrounding tissue.

In vivo administration of either TIM-4-Ig or TIM-1-Ig resulted in hyperproliferation of T cells and enhancement of T cell cytokine production (Meyers et al., 2005). The administration of TIM-1 agonistic mAb enhanced T cell activation and proliferation, induced increased airway inflammation, and blocked development of respiratory tolerance (Umetsu et al., 2005). On T cells, TIM-1 associates with the T cell receptor, and crosslinking with TIM-1 mAb leads to engagement of tyrosine signaling motifs in the cytoplasmic domain of TIM-1 and higher production of Th2 cytokines (Binne et al., 2007; de Souza et al., 2005). A common perplexing feature of in vivo treatment with TIM mAbs or fusion proteins is the finding that at a time when T cells should have returned to quiescence, T cells taken from the treated animal and assayed in vitro are still proliferating and producing cytokines. During a primary T cell response in vivo, T cells expand exponentially and then 90% or more die by apoptosis and are phagocytosed. T cell activation leads to a rise of exposed PS on the surface of the T cell, and this PS is associated with lipid rafts and the immunological synapse (Fischer et al., 2006). Although some in vitro-activated T cells express high levels of PS and progress to activation-induced cell death, the majority express an intermediate level of PS, survive, and restore PS exposure to normal levels. TIM-mediated recognition of PS on activated T cells may have a role as T cells pass through this “near-death” experience. The extended T cell response caused by TIM blockade may be due to prevention of phagocytosis of activated T cells exposing PS. Rapid removal of apoptotic cells by phagocytes is critical for the maintenance of tolerance and

prevents inflammation and autoimmune responses against intracellular antigens released from the dying cells (Savill and Fadok, 2000) (Wu et al., 2006). Disruption of this process may explain the genetic association of the TIM gene family with autoimmunity and asthma.

## EXPERIMENTAL PROCEDURES

### Case Material

Case materials were obtained from the Brigham & Women's Hospital and Dana-Farber Cancer Institute (Boston, MA) after institutional review board (IRB) approval and in accordance with institutional policies.

### Mice

All mouse experiments were approved by the Animal Care and Use Committee of the Dana-Farber Cancer Institute or Children's Hospital Boston. C57BL/6 and BALB/cByJ mice were purchased from Jackson Laboratories. For the collection of resident peritoneal cells, mice were sacrificed and the peritoneal cavities were infused with 3 ml of ice-cold PBS + 0.3% BSA + 0.03% EDTA, and cells were recovered and washed three times in media.

### Generation of Monoclonal Antibodies

BALB/cByJ mice were immunized subcutaneously with human TIM-1(IgV)-Ig or TIM-4(IgV)-Ig in CFA and boosted multiple times with the protein in PBS or IFA. One day after final boost, lymph node cells were fused with NS1 myeloma cells and cloned, and the hybridomas were screened by cell-surface staining of human TIM-1- or TIM-4-transfected 300.19 cells. 3D1 (mouse IgG1) and 1D12 (mouse IgG1) for hTIM-1; 9F4 (mouse IgG1) and 4E11 (mouse IgG2b) for hTIM-4 were chosen. Mouse TIM-1 mAb (3B3, rat IgG2a) has been described (Umetsu et al., 2005). Mouse TIM-4 mAbs (21H12, rat IgG1 and QT3, rat IgG2a) were made by immunization of a Lewis strain rat via a similar protocol and will be described in detail elsewhere (unpublished data). After purification with protein A-Sepharose, antibodies were conjugated to phycoerythrin (PE) by Zymed Laboratories (South San Francisco, CA).

### Ig Fusion Proteins

TIM-Ig fusion proteins (FPs) consist of the complete TIM extracellular domain (indicated as TIM-Ig) or the signal and IgV domain of the TIM [indicated as TIM (IgV)-Ig] linked to the hinge-CH2-CH3 domains of mouse IgG2a (with four point mutations blocking Fc receptor and complement binding) in the pEF6 vector. The mouse TIM-1(IgV) fused to a mouse IgG2a Fc tail (Umetsu et al., 2005) and human TIM-1 fused to a human IgG1 Fc tail (Tami et al., 2007) have been described. Other TIM-Ig were made in the same fashion as mTIM-1(IgV)-Ig (Umetsu et al., 2005). Ig FPs were produced in stably transfected CHO cells and purified from conditioned media by protein A-Sepharose chromatography.

### Cell Transfection

NIH 3T3 cells were transfected by electroporation with a pEF6 plasmid containing hTIM-1 or with wild-type or mutant hTIM-4 cDNAs (W119A, F120A, N121A, D122A). Cells were selected with blasticidin and sorted by flow cytometry for hTIM-1 with 3D1-PE or for hTIM-4 with 9F4-PE or 4E11-PE.

### Mutagenesis

Mutations of a hTIM-4 cDNA in pEF6 were made by oligonucleotide-directed mutagenesis. For example, the D122A mutant was made by PCR amplification of the vector + amino-terminal end and the middle region of hTIM-4 with overlapping primer pairs: 5'-GCTCGGATCCAC TAGTCCAGTGTG-3' with 5'-TTACAGCGTTGAACCAGCCAGGCAC TTCTATG-3' and 5'-CTGGCTGGTTCAACGCTGTAAAGATAAACGT G-3' with 5'-TGTGGCTTCTCCGGAAGGGTGTGGGGTTA-3', respectively. The two PCR fragments were incubated with Spe I- and

BspE I-digested Tim-4 plasmid, joined by In-Fusion assembly (Zhu et al., 2007), and transformed into *E. coli*, and the sequence was confirmed.

### Immunohistochemistry

Immunostaining for TIM-4 was performed on formalin-fixed paraffin-embedded human tissue sections following microwave antigen retrieval in 10 mM citrate buffer, pH 6.0, via a standard indirect avidin-biotin horseradish peroxidase (HRP) method and diaminobenzidine color development, as previously described (Dorfman et al., 2003). Immunostaining with goat anti-human TIM-4 polyclonal antibody (R&D Systems) was compared with that of goat IgG control antibody diluted to identical protein concentration for all cases studied in order to confirm staining specificity. The specificity of TIM-4 immunostaining was also compared after absorption of the TIM-4 antibody on TIM-4-transfected 300.19 cells or untransfected 300.19 cells.

### Transmission Electron Microscopy

HTIM-4-transfected 3T3 cells were incubated with apoptotic U937 for 90 min, washed, and fixed in 0.1M cacodylate buffer (pH 7.4) containing 2.5% formaldehyde, 5% glutaraldehyde, and 0.06% picric acid. Fixed cells were embedded in Epon-araldite and 2.4 volumes of dodecyl succinic anhydride and propylene oxide and hardened at 60°. Thin sections (1 μm or less) were examined with a JEM-1200 EX electron microscope.

### Quantitative RT-PCR

Total RNA was extracted from cells or organs with Trizol (Invitrogen). Human thymus, liver, kidney, lung, and testis RNAs were from multiple-tissue cDNA panels (Clontech). Reverse transcription was done with Taqman reverse-transcription reagents (Applied Biosystems) with Oligo(dT) as the primer, following the manufacturer's protocol. The mouse and human TIM-4 and GAPDH primer-probe sets were purchased from Applied Biosystems. Taqman Universal PCR Master Mix and the 7500 Real-Time PCR System (Applied Biosystems) were used for PCR. Comparative threshold cycles ( $C_T$ ) was used to determine gene expression. For each sample, the TIM-4  $C_T$  value was normalized with the formula  $\Delta C_T = C_{T-TIM-4} - C_{T-GAPDH}$ . For relative expression, the mean  $\Delta C_T$  was determined, and relative TIM-4 expression was calculated with the formula  $2^{-\Delta C_T}$ .

### Preparation of Primary Cells and Cell Separation

Cells from human spleen were obtained by physical disruption followed by filtration through a 70 μm nylon cell strainer (BD Bioscience). Mononuclear cells were separated by Ficoll-Hypaque (GE-Healthcare) and washed with PBS with 2% FBS. CD14<sup>+</sup> and CD14<sup>-</sup> cells were purified through positive selection by MACS Sort magnetic beads in MACS LS Separation columns (Miltenyi Biotec). The percentages of CD14<sup>+</sup> cells were analyzed by flow cytometry with FITC-conjugated human CD14 mAb (BD PharMingen) and were greater than 70% in CD14<sup>+</sup> cells and less than 0.9% in CD14<sup>-</sup> cells. Adherent splenic cells were prepared by culture on tissue-culture plates for 2 hr at 37°C, and nonadherent cells were removed by washing with PBS.

### Flow Cytometry

For determination of cell-surface mTIM-4 expression on freshly isolated cells, cells were preincubated with Fc receptor mAb (2.4G2, ATCC) for 15 min to block Fc receptors. Peritoneal cells were stained with allophycocyanin-conjugated F4/80 mAb (BD PharMingen). CD11c<sup>+</sup> cells were purified by positive selection (using MACS CD11c microbeads [Miltenyi Biotec]) from spleen and stained with PE-Cy5-anti-CD8α (clone 53-6.7). B cells were stained with anti-CD19 (FITC) (BD PharMingen). Cells were costained with PE-conjugated mTIM-4 mAb or isotype control, washed, and analyzed. For determination of TIM-Ig binding, cells were stained with TIM-Ig or isotype control in PBS + 2% FCS + 0.02% NaN<sub>3</sub> for 30 min on ice, washed twice, and then stained with PE- or allophycocyanin-conjugated goat F(ab')<sub>2</sub> anti-mouse IgG2a or PE-conjugated anti-human IgG (Southern

Biotech), depending on FP isotype. For determining whether TIM mAbs blocked binding of TIM-Ig, the indicated TIM-Ig was preincubated with TIM mAb or isotype control for 30 min and then used to stain cells as described above. Flow cytometry was performed on a Cytomics FC500 (Beckman-Coulter), and data were processed with FlowJo software (Tree Star).

#### Preparation of Apoptotic Cells and Eryptotic RBCs

Jurkat cells were cultured for 3 hr in the presence of agonistic anti-human CD95 mAb (7C11, IgM, 1:500 to 1:2000 dilution of ascites) (Robertson et al., 1995). The U937 human monocyte cell line was incubated with 50  $\mu$ M etoposide (Sigma) for 5 hr. Thymocytes from C57BL/6 mice were incubated with 10  $\mu$ M dexamethasone (Sigma) in RPMI for 3 hr. Human RBCs from fresh human blood were separated from plasma, platelets, and PBMCs by Ficoll-Hypaque centrifugation. After centrifugation, neutrophils and the upper 10% of RBCs were removed by pipetting. The remaining RBCs were washed twice and incubated in RPMI containing 4  $\mu$ M ionomycin (Sigma) and 1 mM  $\text{CaCl}_2$  for 3 hr as described previously (Lang et al., 2005). Apoptosis and PS expression on the outer leaflet of the plasma membrane were detected by staining with AnnexinV-FITC and propidium iodide kit (BD PharMingen). After treatment, U937 were washed three times and labeled with 2–5  $\mu$ M of CellTracker Orange (CMTMR, Molecular Probes, FL2 channel) and thymocytes or RBCs with 1–2  $\mu$ M PKH67 (Sigma, FL1 channel) according to the manufacturer's instructions.

#### Phospholipid-Liposome Preparation

Small unilamellar liposomes containing the indicated phospholipids(s) (Avanti Polar Lipids) were made as described previously (Fadok et al., 2000). A plus symbol (PS + PC) indicates a 50:50 molar mix of the indicated lipids. The lipids were mixed in chloroform, dried, resuspended in PBS, mixed, and sonicated for 3 min.

#### Phagocytosis Assay

Resident peritoneal cells ( $1 \times 10^6$ ) were cultured in 24-well plates for 2 hr and washed with PBS three times. mTIM-4 mAb or isotype control was added to the cells in media and preincubated for 5 min before the addition of  $1 \times 10^6$  PKH67-labeled apoptotic thymocytes. After 30 min at 37°C, cells were washed twice with cold PBS and then detached from the plates by treatment with 0.05% trypsin and 0.02% EDTA (Cellgro). Collected cells were stained with PE-conjugated CD11b mAb (BD PharMingen) and analyzed by flow cytometry. CD11b<sup>+</sup> cells that were also PKH67<sup>+</sup> were counted as phagocytic.

Phagocytosis by TIM-transfected 3T3 cells or the human renal clear-cell carcinoma 769P cell line (ATCC) was measured by first culturing  $5 \times 10^4$  cells in 24-well plates for 2 days. Cells were then coincubated with labeled live or apoptotic U937 or fresh or eryptotic RBCs for 45 to 90 min at 37°C. Plates were quickly washed three times with cold PBS with 0.5 mM EDTA to remove nonadherent U937 or RBCs and then detached by treatment with 0.05% trypsin and 0.02% EDTA (Cellgro) and analyzed by flow cytometry. TIM 3T3 or 769P cells were gated by forward and side scatter. For examination of whether liposomes containing PS blocked phagocytosis, cells were preincubated with phospholipid liposomes for 10 min and then incubated with eryptotic RBCs. Where indicated, cells were preincubated with TIM mAb or isotype control for 30 min before the addition of eryptotic RBCs.

Phagocytosis was also evaluated by confocal and fluorescent microscopy. TIM-transfected 3T3 cells or 769P cells ( $5 \times 10^4$ ) were cultured for 2 days in 4-well Lab-Tek II Chamber Slides (Nalge Nunc). Slides were washed one time with RPMI without serum, and cells were labeled with 2–5  $\mu$ M of CellTracker Green (CMFDA, Molecular Probes) in RPMI according to the manufacturer's instructions. Cells were coincubated with CMTMR-labeled U937 for 45 to 90 min. Slides were quickly washed three times with cold PBS with 0.5 mM EDTA and fixed with 3% paraformaldehyde. Samples were analyzed on a Nikon TE2000-U inverted Microscope with EZ-C1 software (Nikon) or an Olympus CKX41.

#### pH-Sensitive Dye Labeling of Apoptotic Cells

Apoptotic U937 were washed three times with PBS, labeled with 2  $\mu$ M CypHer5E Mono NHS ester (GE Healthcare) in PBS for 20 min at room temperature, washed, incubated with hTIM-4-transfected 3T3 cells for 100 min, and washed. Localization of apoptotic bodies from neutral cell surface (colorless) into acidic intracellular endosomes (deep red) was detected by excitation with a 635 nm laser, and emission fluorescence was collected with the Fluoview 1000 spectral scanner (Olympus). Images were manipulated in Volocity (Improvision, Waltham, MA) for presentation in movie format. Photoshop and NIH ImageJ were used to composite images.

#### PIP-Strip Assay

PIP strips on which the indicated phospholipids had been spotted were purchased from Echelon Bioscience. Dot-blot experiments were carried out according to the manufacturer's protocol. Strips were incubated overnight in StartingBlock (TBS) Blocking Buffer (Pierce) at 4°C and then transferred to 2  $\mu$ g/ml of TIM-Ig in blocking buffer with 0.5 mM  $\text{CaCl}_2$  for 2 hr. The PIP strip was then washed three times in TBST (140 mM NaCl, 10 mM Tris-HCl, 0.1% Tween20) with 0.5 mM  $\text{CaCl}_2$  before incubating with HRP-conjugated rat anti-mouse IgG2a mAb (BD PharMingen). Antibody binding was detected with ECL plus western-blotting detection reagents (Amersham Bioscience) and visualized with Kodak X-Omat 2000A processor.

#### Solid-Phase ELISA

The solid-phase ELISA for TIM binding to phospholipids was carried out as described (Hanayama et al., 2002). In brief, the indicated phospholipids in methanol (5  $\mu$ g/ml, 100  $\mu$ l) were added to polystyrene ELISA plates and air-dried. The plates were then blocked with 2% BSA in PBS. TIM-Ig or PS mAb (clone 1H6, mIgG2a, Upstate) were diluted in PBS, added to the wells, and incubated at room temperature for 2 hr. The plates were washed with PBS with 0.05% Tween 20 before incubation with goat F(ab')<sub>2</sub> anti-mouse IgG2a biotin and Streptavidin-HRP (Southern Biotech) for mTIM-1, mTIM-2, mTIM-4, and hTIM-4-Ig or goat anti-human IgG-HRP (Jackson Immunoresearch) for hTIM-1-Ig. The absorbance at 450 nm was measured with Spectra Max190 (Molecular Devices).

#### Supplemental Data

Four figures and one movie are available at <http://www.immunity.com/cgi/content/full/27/6/927/DC1/>.

#### ACKNOWLEDGMENTS

We express our thanks to Michael Robertson and Jerry Ritz for anti-Fas mAb and to Barbara Seaton for helpful discussions on PS receptors. This work was supported by NIH P01 AI054456 (to G.J.F., D.T.U., G.G.K., and R.D.K.) and NIH R01 NS045937 (to G.J.F.).

Received: July 26, 2007

Revised: October 31, 2007

Accepted: November 19, 2007

Published online: December 13, 2007

#### REFERENCES

- Asano, K., Miwa, M., Miwa, K., Hanayama, R., Nagase, H., Nagata, S., and Tanaka, M. (2004). Masking of phosphatidylserine inhibits apoptotic cell engulfment and induces autoantibody production in mice. *J. Exp. Med.* 200, 459–467.
- Balasubramanian, K., Chandra, J., and Schroit, A.J. (1997). Immune clearance of phosphatidylserine-expressing cells by phagocytes. The role of beta2-glycoprotein I in macrophage recognition. *J. Biol. Chem.* 272, 31113–31117.

- Beletskii, A., Cooper, M., Sriraman, P., Chiriac, C., Zhao, L., Abbot, S., and Yu, L. (2005). High-throughput phagocytosis assay utilizing a pH-sensitive fluorescent dye. *Biotechniques* 39, 894–897.
- Binne, L.L., Scott, M.L., and Rennert, P.D. (2007). Human TIM-1 associates with the TCR complex and up-regulates T cell activation signals. *J. Immunol.* 178, 4342–4350.
- Borisenko, G.G., Matsura, T., Liu, S.X., Tyurin, V.A., Jianfei, J., Serinkan, F.B., and Kagan, V.E. (2003). Macrophage recognition of externalized phosphatidylserine and phagocytosis of apoptotic Jurkat cells—existence of a threshold. *Arch. Biochem. Biophys.* 413, 41–52.
- Cao, E., Zang, X., Ramagopal, U.A., Mukhopadhyaya, A., Fedorov, A., Fedorov, E., Zencheck, W.D., Lary, J.W., Cole, J.L., Deng, H., et al. (2007). T cell immunoglobulin mucin-3 crystal structure reveals a galectin-9-independent ligand-binding surface. *Immunity* 26, 311–321.
- Cohen, P.L., Caricchio, R., Abraham, V., Camenisch, T.D., Jennette, J.C., Roubey, R.A., Earp, H.S., Matsushima, G., and Reap, E.A. (2002). Delayed apoptotic cell clearance and lupus-like autoimmunity in mice lacking the c-mer membrane tyrosine kinase. *J. Exp. Med.* 196, 135–140.
- de Souza, A.J., Oriss, T.B., O'Malley, K.J., Ray, A., and Kane, L.P. (2005). T cell Ig and mucin 1 (TIM-1) is expressed on in vivo-activated T cells and provides a costimulatory signal for T cell activation. *Proc. Natl. Acad. Sci. USA* 102, 17113–17118.
- Dorfman, D.M., Greisman, H.A., and Shahsafaei, A. (2003). Loss of expression of the WNT/beta-catenin-signaling pathway transcription factors lymphoid enhancer factor-1 (LEF-1) and T cell factor-1 (TCF-1) in a subset of peripheral T cell lymphomas. *Am. J. Pathol.* 162, 1539–1544.
- Fadok, V.A., Voelker, D.R., Campbell, P.A., Cohen, J.J., Bratton, D.L., and Henson, P.M. (1992). Exposure of phosphatidylserine on the surface of apoptotic lymphocytes triggers specific recognition and removal by macrophages. *J. Immunol.* 148, 2207–2216.
- Fadok, V.A., Bratton, D.L., Rose, D.M., Pearson, A., Ezekewitz, R.A., and Henson, P.M. (2000). A receptor for phosphatidylserine-specific clearance of apoptotic cells. *Nature* 405, 85–90.
- Fischer, K., Voelkl, S., Berger, J., Andreesen, R., Pomorski, T., and Mackensen, A. (2006). Antigen recognition induces phosphatidylserine exposure on the cell surface of human CD8+ T cells. *Blood* 108, 4094–4101.
- Han, W.K., Bailly, V., Abichandani, R., Thadhani, R., and Bonventre, J.V. (2002). Kidney Injury Molecule-1 (KIM-1): A novel biomarker for human renal proximal tubule injury. *Kidney Int.* 62, 237–244.
- Hanayama, R., Tanaka, M., Miwa, K., Shinohara, A., Iwamatsu, A., and Nagata, S. (2002). Identification of a factor that links apoptotic cells to phagocytes. *Nature* 417, 182–187.
- Ichimura, T., Bonventre, J.V., Bailly, V., Wei, H., Hession, C.A., Cate, R.L., and Sanicola, M. (1998). Kidney injury molecule-1 (KIM-1), a putative epithelial cell adhesion molecule containing a novel immunoglobulin domain, is up-regulated in renal cells after injury. *J. Biol. Chem.* 273, 4135–4142.
- Kuchroo, V.K., Umetsu, D.T., DeKruyff, R.H., and Freeman, G.J. (2003). The TIM gene family: Emerging roles in immunity and disease. *Nat. Rev. Immunol.* 3, 454–462.
- Kuchroo, V.K., Meyers, J.H., Umetsu, D.T., and DeKruyff, R.H. (2006). TIM family of genes in immunity and tolerance. *Adv. Immunol.* 91, 227–249.
- Lang, K.S., Lang, P.A., Bauer, C., Duranton, C., Wieder, T., Huber, S.M., and Lang, F. (2005). Mechanisms of suicidal erythrocyte death. *Cell. Physiol. Biochem.* 15, 195–202.
- McIntire, J.J., Umetsu, S.E., Akbari, O., Potter, M., Kuchroo, V.K., Barsh, G.S., Freeman, G.J., Umetsu, D.T., and DeKruyff, R.H. (2001). Identification of Tapr (an airway hyperreactivity regulatory locus) and the linked Tim gene family. *Nat. Immunol.* 2, 1109–1116.
- Meyers, J.H., Chakravarti, S., Schlesinger, D., Illes, Z., Waldner, H., Umetsu, S.E., Kenny, J., Zheng, X.X., Umetsu, D.T., DeKruyff, R.H., et al. (2005). TIM-4 is the ligand for TIM-1, and the TIM-1-TIM-4 interaction regulates T cell proliferation. *Nat. Immunol.* 6, 455–464.
- Monney, L., Sabatos, C.A., Gaglia, J.L., Ryu, A., Waldner, H., Chernova, T., Manning, S., Greenfield, E.A., Coyle, A.J., Sobel, R.A., et al. (2002). Th1-specific cell surface protein Tim-3 regulates macrophage activation and severity of an autoimmune disease. *Nature* 415, 536–541.
- Nagata, K., Ohashi, K., Nakano, T., Arita, H., Zong, C., Hanafusa, H., and Mizuno, K. (1996). Identification of the product of growth arrest-specific gene 6 as a common ligand for Axl, Sky, and Mer receptor tyrosine kinases. *J. Biol. Chem.* 271, 30022–30027.
- Nakano, T., Ishimoto, Y., Kishino, J., Umeda, M., Inoue, K., Nagata, K., Ohashi, K., Mizuno, K., and Arita, H. (1997). Cell adhesion to phosphatidylserine mediated by a product of growth arrest-specific gene 6. *J. Biol. Chem.* 272, 29411–29414.
- Oka, K., Sawamura, T., Kikuta, K., Itokawa, S., Kume, N., Kita, T., and Masaki, T. (1998). Lectin-like oxidized low-density lipoprotein receptor 1 mediates phagocytosis of aged/apoptotic cells in endothelial cells. *Proc. Natl. Acad. Sci. USA* 95, 9535–9540.
- Robertson, M.J., Manley, T.J., Pichert, G., Cameron, C., Cochran, K.J., Levine, H., and Ritz, J. (1995). Functional consequences of APO-1/Fas (CD95) antigen expression by normal and neoplastic hematopoietic cells. *Leuk. Lymphoma* 17, 51–61.
- Santiago, C., Ballesteros, A., Martinez-Munoz, L., Mellado, M., Kaplan, G.G., Freeman, G.J., and Casanovas, J.M. (2007a). Structures of T cell immunoglobulin mucin protein 4 show a metal-ion-dependent ligand binding site where phosphatidylserine binds. *Immunity* 27, this issue, 941–951.
- Santiago, C., Ballesteros, A., Tami, C., Martinez-Munoz, L., Kaplan, G.G., and Casanovas, J.M. (2007b). Structures of T cell immunoglobulin mucin receptors 1 and 2 reveal mechanisms for regulation of immune responses by the TIM receptor family. *Immunity* 26, 299–310.
- Savill, J., and Fadok, V. (2000). Corpse clearance defines the meaning of cell death. *Nature* 407, 784–788.
- Scott, R.S., McMahon, E.J., Pop, S.M., Reap, E.A., Caricchio, R., Cohen, P.L., Earp, H.S., and Matsushima, G.K. (2001). Phagocytosis and clearance of apoptotic cells is mediated by MER. *Nature* 411, 207–211.
- Shakhov, A.N., Rybtsov, S., Tumanov, A.V., Shulenin, S., Dean, M., Kuprash, D.V., and Nedospasov, S.A. (2004). SMUCKLER/TIM4 is a distinct member of TIM family expressed by stromal cells of secondary lymphoid tissues and associated with lymphotoxin signaling. *Eur. J. Immunol.* 34, 494–503.
- Sizing, I.D., Bailly, V., McCoon, P., Chang, W., Rao, S., Pablo, L., Rennard, R., Walsh, M., Li, Z., Zafari, M., et al. (2007). Epitope-dependent effect of anti-murine TIM-1 monoclonal antibodies on T cell activity and lung immune responses. *J. Immunol.* 178, 2249–2261.
- Smith, J.P., Lister, A.M., Tew, J.G., and Szakal, A.K. (1991). Kinetics of the tingible body macrophage response in mouse germinal center development and its depression with age. *Anat. Rec.* 229, 511–520.
- Tami, C., Silberstein, E., Manangeeswaran, M., Freeman, G.J., Umetsu, S.E., DeKruyff, R.H., Umetsu, D.T., and Kaplan, G.G. (2007). Immunoglobulin A (IgA) is a natural ligand of hepatitis A virus cellular receptor 1 (HAVCR1), and the association of IgA with HAVCR1 enhances virus-receptor interactions. *J. Virol.* 81, 3437–3446.
- Umetsu, S.E., Lee, W.L., McIntire, J.J., Downey, L., Sanjanwala, B., Akbari, O., Berry, G.J., Nagumo, H., Freeman, G.J., Umetsu, D.T., and DeKruyff, R.H. (2005). TIM-1 induces T cell activation and inhibits the development of peripheral tolerance. *Nat. Immunol.* 6, 447–454.
- Verhoven, B., Schlegel, R.A., and Williamson, P. (1995). Mechanisms of phosphatidylserine exposure, a phagocyte recognition signal, on apoptotic T lymphocytes. *J. Exp. Med.* 182, 1597–1601.

## TIM-4 Binds Phosphatidylserine on Apoptotic Cells

Vila, M.R., Kaplan, G.G., Feigelstock, D., Nadal, M., Morote, J., Porta, R., Bellmunt, J., and Meseguer, A. (2004). Hepatitis A virus receptor blocks cell differentiation and is overexpressed in clear cell renal cell carcinoma. *Kidney Int.* *65*, 1761–1773.

Wilker, P.R., Sedy, J.R., Grigura, V., Murphy, T.L., and Murphy, K.M. (2007). Evidence for carbohydrate recognition and homotypic and heterotypic binding by the TIM family. *Int. Immunol.* *19*, 763–773.

Williamson, P., and Schlegel, R.A. (2004). Hide and seek: The secret identity of the phosphatidylserine receptor. *J. Biol.* *3*, 14.

Wu, Y., Tibrewal, N., and Birge, R.B. (2006). Phosphatidylserine recognition by phagocytes: A view to a kill. *Trends Cell Biol.* *16*, 189–197.

Zhu, B., Cai, G., Hall, E.O., and Freeman, G.J. (2007). In-fusion assembly: seamless engineering of multidomain fusion proteins, modular vectors, and mutations. *Biotechniques* *43*, 354–359.